FULLBAND ENSEMBLE MONTE CARLO MODELING OF HIGH-FIELD TRANSPORT IN THE ZnS PHOSPHOR OF AC THIN FILM ELECTROLUMINESCENT DEVICES

Shankar S. Pennathur, Keya Bhattacharrya, John F. Wager, and Stephen M. Goodnick
Department of Electrical and Computer Engineering
Oregon State University, Corvallis, OR 97331-3211

Abstract

A fullband ensemble Monte Carlo investigation of high-field transport in the ZnS phosphor of ac thin-film electroluminescent (ACTFEL) devices is presented. A full band dispersion computed using empirical pseudopotentials is used to model the first two conduction bands in ZnS. Computed electron energy distributions at high fields reveal a reasonable fraction of electrons energetic enough to impact-excite luminescent centers in the phosphor layer.

I. INTRODUCTION

Alternating current thin-film electroluminescent devices are used in the production of high-resolution, flat-screen displays and are being increasingly researched [1-5]. An ACTFEL device essentially consists of a wide bandgap semiconductor such as ZnS (referred to as the phosphor layer) sandwiched between two insulating layers. Carriers that are sourced into the semiconductor by surface states in the semiconductor-insulator interface, are accelerated under the influence of very high electric fields. The energetic electrons traversing the phosphor layer are then responsible for impact exciting the (intentionally introduced) luminescent centers. Luminescence is obtained as the excited electron states in these centers radiatively relax to their ground states. An understanding of the high-field carrier transport in the phosphor layer and the physics of the different threshold processes such as band-to-band impact ionization and impact excitation of luminescent impurities is essential for device design, especially when newer phosphors are being continually developed in the quest for a full-color EL display.

In this paper, we present the results obtained using a full band model for ZnS for fields in the range 1-2 MV/cm. By including band-to-band impact ionization as well as impact excitation of Mn^{2+} centers, a unified picture of the physical processes crucial to electroluminescence is achieved.

II. MONTE CARLO MODEL

We use a full band dispersion for ZnS, computed using empirical (local) pseudopotentials[6]. The first two conduction bands included in the simulation, span in energy to values sufficiently higher than the most energetic electrons encountered for the electric fields considered. The low-energy scattering rates are computed using a non-parabolic dispersion for the different valleys in the first conduction band. The scattering rates however are corrected at higher energies using the full band density of states thereby forcing the scattering rates to behave as the density of states. Figure 1 shows the total scattering rates computed in the Γ valley of ZnS at 300K. While polar-optic phonon scattering is the dominant scattering mechanism at low energies, intervalley scattering mechanism becomes important beyond 1.5 eV (which is roughly the energy separation between the Γ valley and the X and L valleys). Other scattering mechanisms included in the model are ionized impurity scattering, acoustic phonon scattering, band-to-band impact ionization (at high energies), and impact excitation of Mn^{2+}. Impact ionization is included in the model using a simple Keldysh formulation [7], which specifies the ionization rate as,

$$\Gamma_{ii}(E) = \Gamma_{ph}(E_{th})\, P\, (\frac{E - E_{th}}{E_{th}})^2 \qquad (1)$$

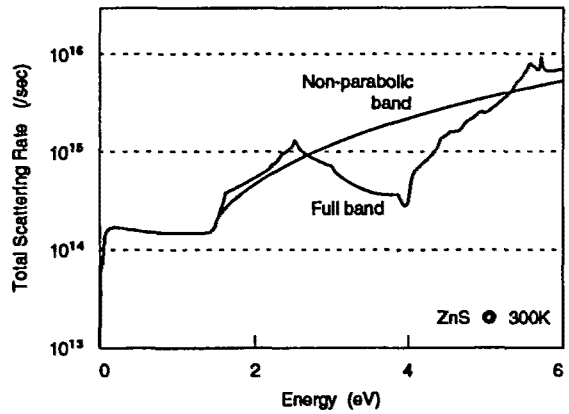

Figure 1: Total scattering rate in the central valley of ZnS at 300 K. Rates for non-parabolic band and adjusted rates for fullband are shown.

where Γ_{ii}, the energy dependent impact ionization rate is proportional to $\Gamma_{ph}(E_{th})$, the total phonon scattering rate at E_{th}, the threshold energy for impact ionization, given as

$$E_{th} = \frac{2m_e + m_h}{m_e + m_h} E_G \tag{2}$$

where m_e, m_h and E_G are the electron and hole band edge effective masses and the energy gap respectively. Our work included a threshold (computed as above) of 4.3 eV and the value of P used was 100. Figure 2 shows the variation of the impact ionization coefficient α_{ii} with the inverse of the electric field, obtained from the Monte Carlo model, fitted to reported experimental values [8] by tuning the deformation potentials for intervalley phonon scattering in the second band, showing a reasonable fit in the electric field values of most interest. Impact excitation is the process in

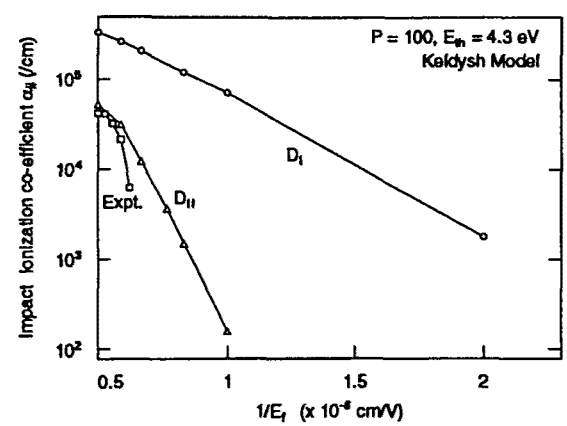

Figure 2: Plot of impact ionization coefficient α_{ii} as a function of inverse electric field. Plots D_I and D_{II} correspond to two different sets of deformation potentials for phonon scattering in the second band.

which a hot electron interacts with a luminescent impurity in the host phosphor, to excite valence electrons in the luminescent center to excited states, losing energy in the process. In this work, we

model the excitation cross-section for a center with a threshold energy E_{ie} as [9]

$$\sigma(E) = \frac{c^2 e^4}{4\pi\epsilon_\infty^2 E^2}\sqrt{\frac{E - E_{ie}}{E}} \tag{3}$$

where e is the electronic charge, and ϵ_∞ is the high frequency dielectric constant. The constant factor c^2 is related to the overlap integral between the hot electron and the interacting impurity's electron wavefunctions, and was fitted to obtain a peak value of $1\times10^{-15}\text{cm}^2$ for the cross-section. The associated scattering rate is then simply given as

$$\Gamma_{ie} = \sigma(E) v_d N_{li} \tag{4}$$

where v_d is the average velocity of the carriers, and N_{li} the density of the centers in the host phosphor (typically about 0.5 atomic %).

III. RESULTS AND DISCUSSION

Figure 3 shows the energy distribution of electrons for three different (typical) phosphor fields, along with the excitation cross-section (in arbitrary units) of Mn^{2+} ions. It is observed that the distribution gets hotter (increasing average energies) with increasing phosphor fields. For Mn^{2+} centers (used for yellow luminescence) with an excitation threshold energy of about 2.1 eV, it is seen that a considerable number of electrons in the ensemble are energetic enough to cause impact excitation. By counting the number of impact excitation events occurring during the simulation

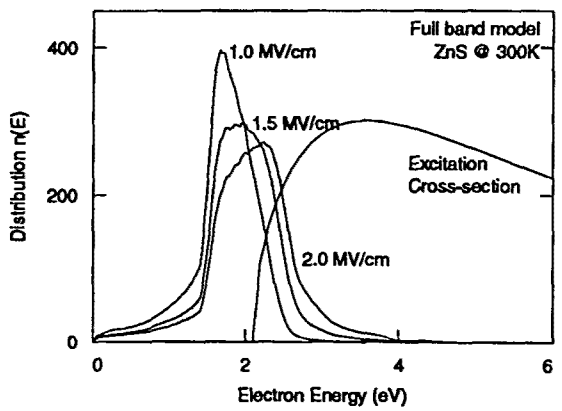

Figure 3: Electron energy distribution at three different phosphor fields plotted along with the excitation cross-section of Mn^{2+} centers.

at steady state over a length of time, an estimate is obtained of the average number of impact excitations effected by an electron as it traverses the entire length of the phosphor layer. This parameter is linked to the maximum observable brightness of the devices. Figure 4 shows a plot of this internal quantum yield parameter as a function of the phosphor field, revealing an almost linear variation, and the existence of a possible cutoff field as the lower limit. Figure 4 also shows the variation of the number of ionization events per transferred electron. There are few ionization events for fields below 1.5 MV/cm, but a significant number of events is observed at higher fields. This variation is consistent with the threshold energies of the impact excitation and impact ionization processes being 2.1 eV and 4.3 eV respectively.

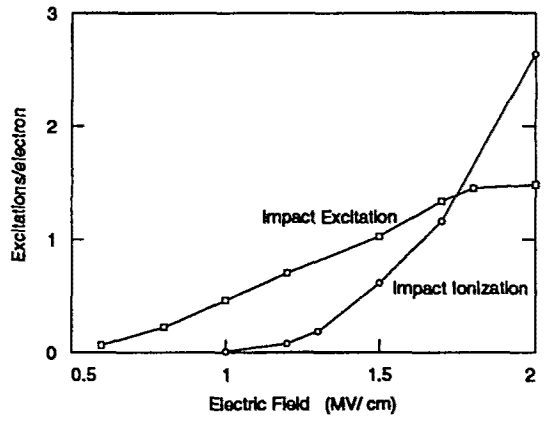

Figure 4: Plot of recorded impact ionization and impact excitations events per transferred electron as a function of the phosphor field.

IV. CONCLUSIONS

A full band Monte Carlo modeling of ZnS phosphor in ACTFEL devices reveals that band-to-band impact ionization plays a crucial role in stabilizing the electron distributions. The steady state electron energy distributions obtained for different phosphor fields reveal a significant fraction of the electrons energetic enough to participate in impact exciting luminescent centers in the host phosphor. Increasing phosphor fields results in hotter energy distributions and relatedly, the estimated internal quantum yield varies linearly with the phosphor field. Impact excitation processes while being the basis of the functionality of these devices do not affect the hot electron energy distributions to any significant degree.

ACKNOWLEDGMENT

The usage of the supercomputing resources of Sandia National Laboratories and NCSA at University of Illinois, in performing the simulations presented in this work, is acknowledged. We thank Dr. Ravaioli at University of Illinois, and Dr. P. Vogl of Walter Schottky Institute, Munich, for their assistance, and Dr. Bringuier for use of his unpublished results. We also acknowledge the support of the U.S. Army Research Office under Contract No. D11L03-91G0242.

REFERENCES

[1] B. K. Ridley, *J. Phys. C: Solid State Phys.*, **16**, 3373 (1983).

[2] E. Bringuier, *J. Appl. Phys.*, **70**, 4505, 1991.

[3] R. Mach and G. O. Müller, *J. Cryst. Growth*, **101**, 967, 1990.

[4] K. Bhattacharyya, S. M. Goodnick, and J. F. Wager, *J. Appl. Phys.*, **73**, 3390, 1993.

[5] K. Brennan, *J. Appl. Phys.*, **64**, 4024, 1988.

[6] M. L. Cohen and T. K. Bergstresser, *Phys. Rev.*, **166**, 789, 1966.

[7] L. V. Keldysh, *Sov. Phys. JETP*, **21**, 1135, 1965.

[8] T. D. Thompson and J. W. Allen, *J. Phys. C: Solid State Phys.*, **20**, L499, 1987.

[9] E. Bringuier and K. Bhattacharyya, Unpublished work.